Note: This copy is for your personal non-commercial use only. To order presentation-ready copies for distribution to your colleagues or clients, contact us at www.rsna.org/rsnarights.

RadioGraphics

AAPM/RSNA Physics Tutorial for Residents

MR Artifacts, Safety, and Quality Control[1]

Jiachen Zhuo, MS • Rao P. Gullapalli, PhD

TEACHING POINTS
See last page

Artifacts in magnetic resonance (MR) imaging result from the complex interaction of contemporary imager subsystems, including the main magnet, gradient coils, radiofrequency (RF) transmitter and receiver, and reconstruction algorithm used. An understanding of the sources of artifacts enables optimization of the MR imaging system performance. The increasing clinical use of very high magnetic field strengths, high-performance gradients, and multiple RF channels also mandates renewed attention to the biologic effects and physical safety of MR imaging. Radiologists should be aware of the potential physiologic effects of prolonged exposure to magnetic fields, acoustic noise, and RF energy during MR imaging and should use all the available methods for avoiding accidents and adverse effects. Imaging equipment should be regularly tested and monitored to ensure its stability and the uniformity of its functioning. Newly installed or upgraded MR systems should be tested by a physicist or qualified engineer before use. In addition, the authors recommend participation in the MR imaging accreditation program of the American College of Radiology to establish the initial framework for an adequate quality assurance program, which then can be further developed to fulfill local institutional needs.

©RSNA, 2006

Abbreviations: ACR = American College of Radiology, FDA = Food and Drug Administration, GRE = gradient-recalled echo, RF = radiofrequency, SE = spin echo, STIR = short inversion time inversion recovery, 3D = three-dimensional

RadioGraphics 2006; 26:275–297 • **Published online** 10.1148/rg.261055134 • **Content Codes:** MR PH QA

[1]From the Department of Radiology, University of Maryland School of Medicine, 22 S Greene St, Baltimore, MD 21201. From the AAPM/RSNA Physics Tutorial for Residents at the 2004 RSNA Annual Meeting. Received June 27, 2005; revision requested September 16 and received October 13; accepted October 14. All authors have no financial relationships to disclose. **Address correspondence to** R.P.G. (e-mail: *rgullapalli@umm.edu*).

©RSNA, 2006

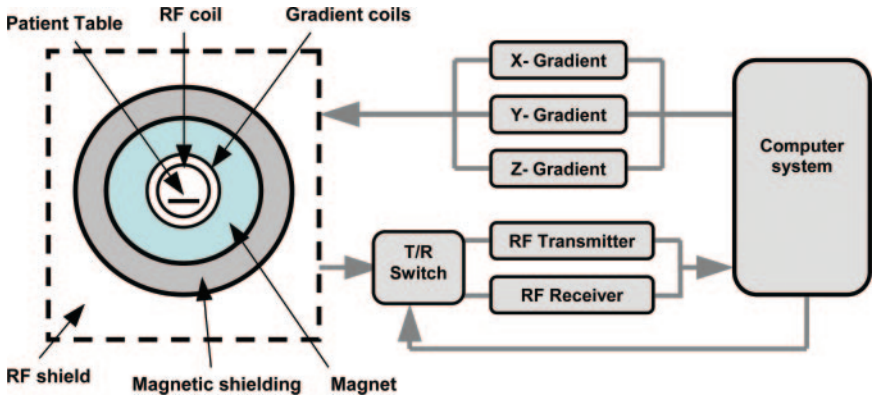

Figure 1. Schematic shows the basic components and architecture of an MR imaging system. *T/R* = transmit-receive.

Introduction

Since the invention of magnetic resonance (MR) imaging in 1972, the field has grown by leaps and bounds (1). Today, MR imaging is available in small community hospitals, in the far corners of the country, and in many private outpatient clinics. The large growth in this field is attributable to rapid technologic advances in several areas, including magnet technology, gradient coil design, radiofrequency (RF) technology, and computer engineering. In stride with the rapid technologic advances, there has been phenomenal growth in the number of applications for MR imaging. We no longer look to MR imaging to provide only structural information, but also functional information of various kinds. Information about blood flow, cardiac function, biochemical processes, tumor kinetics, and blood oxygen levels (for mapping of brain function) are just a few examples of the data that can be obtained with MR imaging today (2–6).

Teaching Point

Since the first U.S. Food and Drug Administration (FDA)-approved MR imaging system arrived in the marketplace around 30 years ago, the available magnetic field strengths have increased 20-fold and more, the gradient capabilities have increased 100- to 200-fold, and the RF chain has been completely revamped with phased-array coil imaging and parallel imaging (7,8). We have gone from the single receiver to the quadrature coil, to multielement fast receivers. The growing demand for new applications has helped to fuel rapid growth in the number and type of pulse sequences available to radiologists. Imaging techniques have progressed from the simple spin-echo (SE) sequence to include steady-state, fast SE, echo-planar, and parallel imaging sequences (9,10). At the same time, radiologists and clinicians have had to adjust to the pace of change. They have had to learn to apply these new techniques and to distinguish between clinical features and potential artifacts on the resultant images.

Demands for higher spatial and temporal resolution for both structural and functional imaging have led to the proliferation of higher magnetic field strengths. Over the past 5 years, ultra-high-field-strength magnets (>1.5 T) have taken the market by storm and have quickly moved from a research environment to a clinical environment. The high magnetic field strengths and the high-performance gradients have brought a new awareness of the issue of safety for both clinicians and patients. The effects of exposure to magnetic fields and the compatibility of the many so-called MR-compatible or MR-safe surgical implants and other tools are being reinvestigated at high field strengths. The use of rapid imaging techniques such as echo-planar imaging and half-Fourier rapid acquisition with relaxation enhancement, or RARE, along with the use of ultra-high-speed gradients, has raised awareness and concern for the biologic effects of exposure.

With the expansion of the array of applications and increased number of users, it has become necessary to institute measures for quality control over the daily operations of MR imaging centers. The effort to control quality has been spearheaded mainly by the American College of Radiology (ACR), which has instituted a program for certification in MR imaging. Although certification is voluntary, more and more payers of clinical MR imaging costs are basing their payments on whether a site is ACR accredited or not.

The different components of an MR imaging system are shown in Figure 1. The main subsystems are the magnet, gradient coil, RF generator, and computer, the last of which controls the interplay between subsystems and the reconstruction, storage, and display of the images. There are many sources of artifacts on MR images. These could broadly be classified as image reconstruction–related, system-related, and physiology-related sources. Typically, image reconstruction–related artifacts occur because of limitations intrinsic to the reconstruction algorithm used by the

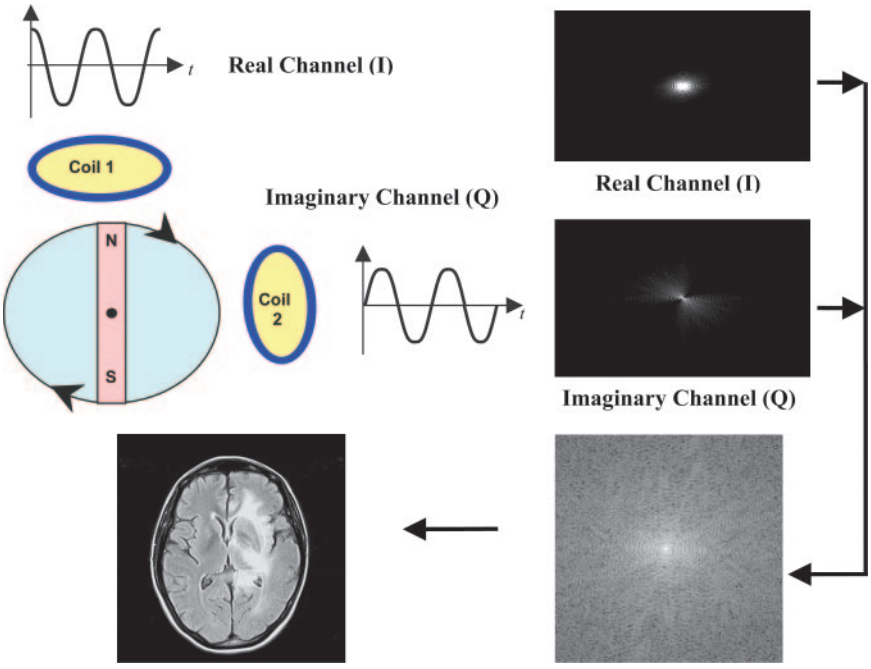

Figure 2. Schematic of quadrature coil detection shows the collection and combination of real and imaginary MR signal data to produce a complex map of k-space, which is then subjected to Fourier analysis to obtain the MR image.

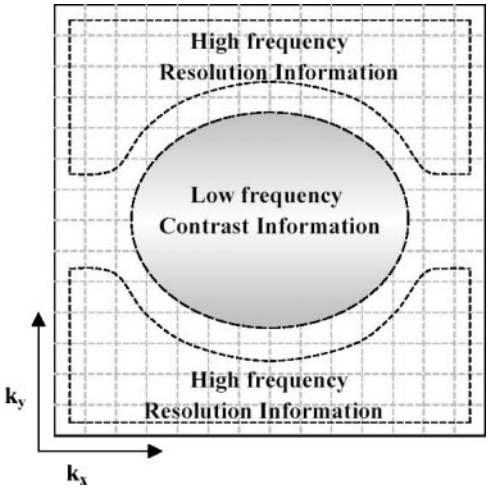

Figure 3. Schematic shows the location of low-frequency information about image contrast resolution at the center of k-space, and, at the edges of k-space, high-frequency information about spatial resolution and fine structure.

particular vendor. System-related artifacts might be due to transient effects generated within one or more of the subsystems or could be a sign of degradation of some of the electronic components in the subsystem. System-related artifacts can be minimized through the adoption of a good quality assurance or quality control program, such as the one recommended by the ACR. Artifacts related to physiology are dependent on complex interactions between the subject and the MR imaging system. These include artifacts due to breathing-related or other motion of the subject, as well as flow-related artifacts. Physiology-related artifacts may be minimized with an understanding of the basic anatomy and physiology involved and the appropriate use of specific pulse sequences.

Teaching Point

The next section, a brief overview of k-space, is followed by a discussion of the types of common artifacts seen on MR images. Safety concerns related to MR imaging are discussed according to subsystem, and guidelines for practice safety in the MR imaging workplace are provided. Finally, the authors suggest some basic quality assurance procedures that may help to minimize artifacts and increase system uptime while maintaining high quality.

k-Space

MR imaging systems collect data over time. The data that are captured during MR imaging are called k-space data or, simply, raw data. Typically, the data are collected by using quadrature detection, which provides both real and imaginary k-space data. k-Space data include useful information but can be interpreted only after they are translated into images with the Fourier transform method (Fig 2). Several types of motion may occur during the collection of k-space data. The motion may cause artifacts, which represent the complex interaction between the motion and the data acquisition time. Hence, an understanding of k-space is a critical element in the understanding and possible elimination of motion artifacts.

The process of k-space detection and image acquisition is shown in Figure 2, and the typical characteristics of k-space are shown in Figure 3.

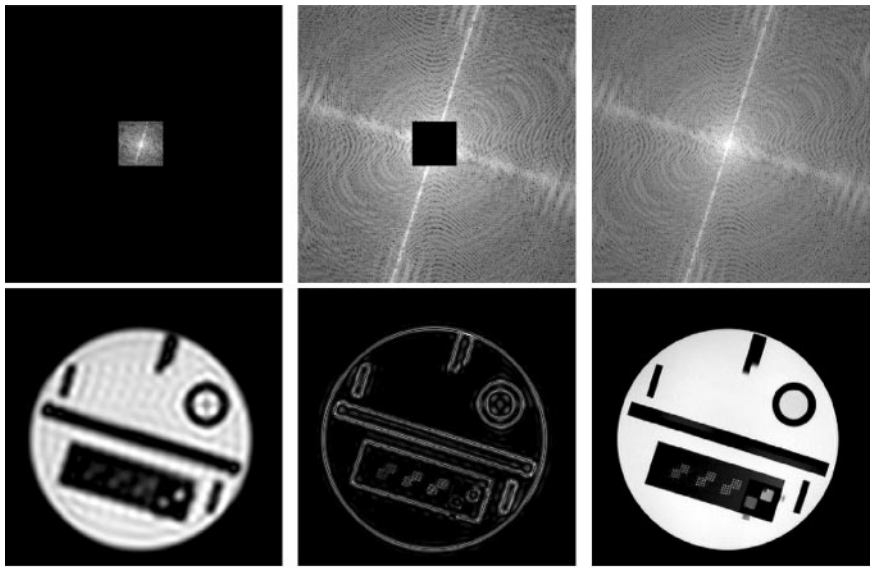

Figure 4. Maps of k-space data (top row) and corresponding MR images (bottom row) obtained in a phantom illustrate the relationship between raw k-space data and the reconstructed MR image after Fourier transform. **(a)** Image reconstructed only with data from the center of k-space has high contrast but low spatial resolution (poor definition). **(b)** Image reconstructed only with data from the periphery of k-space shows well-defined edges but has poor contrast resolution. **(c)** Image reconstructed with all the k-space data has both good contrast and good spatial resolution.

As mentioned earlier, k-space is the rawest form of data obtained at MR imaging. An acquisition with a 256 × 256 matrix contains 256 lines of data, and each of those lines contains 256 data points. The y-dimension in this 256 × 256 array is called the phase encoding direction, and the x-dimension is called the frequency encoding direction. The distance between neighboring points in k-space determines the field of view of the object imaged, and the extent of k-space determines the resolution of the image. For a matrix with the same resolution, sparse sampling of the points would require less gradient strength and would produce images with a larger field of view, whereas faster sampling of points would require a higher gradient strength and would produce images with a smaller field of view. Filling of k-space is accomplished by acquiring frequency encoded data samples for a given phase encoding step. Sampling is much quicker in the frequency encoding direction than in the phase encoding direction, where the time between adjacent samples is greater than or equal to the repetition time of the particular sequence (except for fast SE and echo-planar imaging sequences). Low spatial frequencies are encoded in the center of k-space and provide contrast resolution to the image, whereas high spatial frequencies are encoded toward the edges of k-space and contribute to the spatial resolution of the image (11,12) (Fig 4). Fourier transform of k-space is then applied to convert the data into an image. Each pixel in the resultant image is the weighted sum of all the individual points in k-space. Therefore, the information in each pixel is derived from a fraction of every point in k-space. On the basis of these facts, we can conclude that any disruption of k-space, whether by motion, extraneous frequencies, or frequency spikes, has the potential to corrupt the entire image. In the next section, we describe the types of artifacts that might appear on MR images.

Teaching Point

Equipment-related Artifacts

Spike (Herringbone) Artifact

Gradients applied at a very high duty cycle (eg, those in echo-planar imaging) may produce bad data points, or a spike of noise, in k-space. The bad data might be a single point or a few points in k-space that have a very high or low intensity compared with the intensity of the rest of k-space. The convolution of this spike with all the other image information during the Fourier transform results in dark stripes overlaid on the image

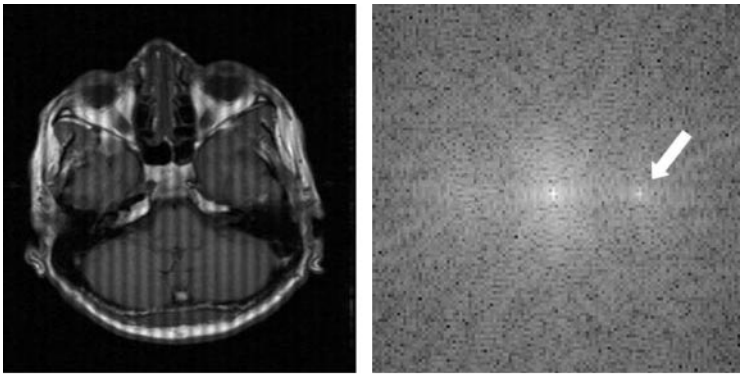

a. b.

Figure 5. Spike artifact. Bad data points in k-space (arrow in **b**) result in band artifacts on the MR image in **a**. The location of the bad data points, and their distance from the center of k-space, determine the angulation of the bands and the distance between them. The intensity of the spike determines the severity of the artifact.

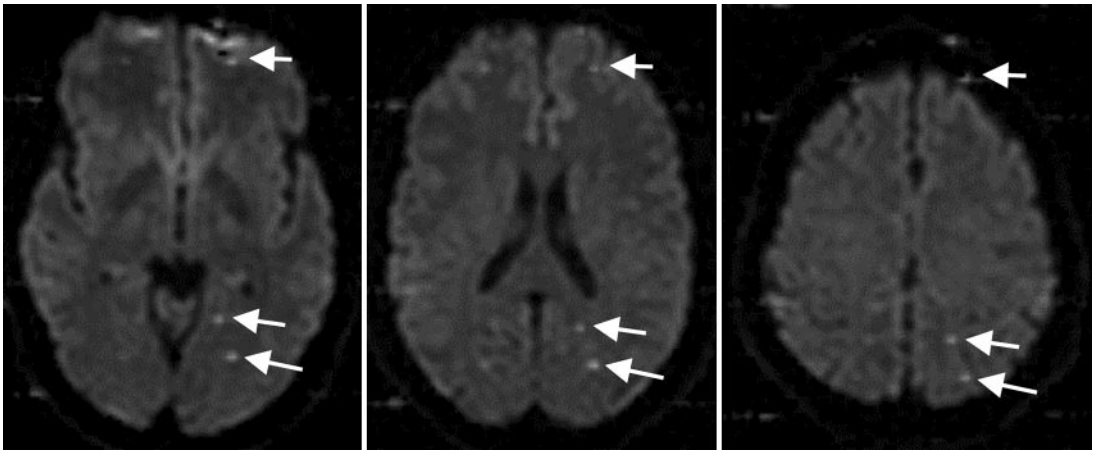

Figure 6. Zipper artifact (RF leakage artifact). Images show constant-frequency artifacts (arrows) produced by RF leakage from electronic components brought into the magnet room.

(Fig 5). The displacement of the spike of noise from the center of k-space determines the spacing between the stripes and the angulation of the stripes with respect to the readout direction. Spike noise usually is transient, but if it is not attended to, it can become chronic. Spike noise usually occurs because of loose electrical connections that produce arcs or because of the breakdown of interconnections in an RF coil, and it is more evident with the use of high-duty-cycle sequences (13).

On the other hand, the pattern of stripes produced by a spike in k-space can be used for tagging, an important technique in cardiac imaging. In this scheme, preparation pulses are applied prior to the imaging sequence. The preparation pulse has an excitation profile such that it forms echoes in different parts of the k-space. Fourier transform of such images produces tags in a grid-like pattern, with known spacing between the stripes. In cardiac imaging, these tags are applied at the start of each cardiac phase, and cardiac image acquisition then is performed at multiple phases of the cardiac cycle. Following the changes in tag position during the cardiac cycle from the point of initial placement can be useful for assessing cardiac motion (14).

Zipper Artifact

The zipper artifact is a common equipment-related artifact caused by the leakage of electromagnetic energy into the magnet room. It appears as a region of increased noise with a width of 1 or 2 pixels that extends in the frequency encoding direction, throughout the image series (Fig 6). All magnet rooms are shielded to eliminate interference from local RF broadcasting stations or from electronic equipment that emits an

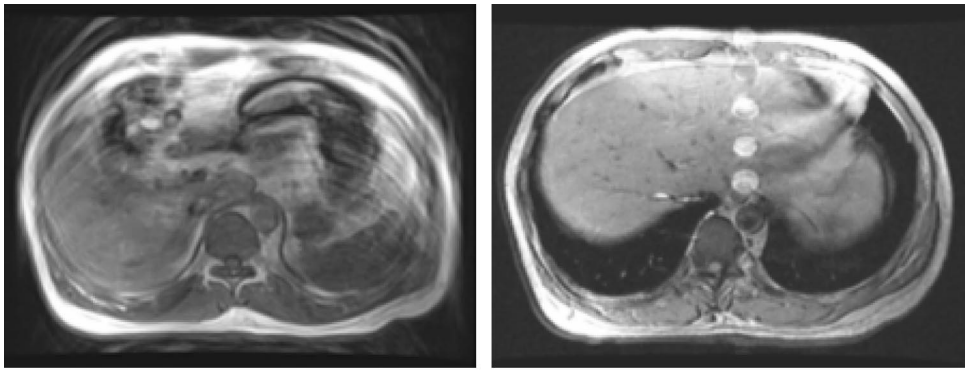

a. b.

Figure 7. Motion-related artifacts. **(a)** Abdominal image obtained without breath hold shows breathing-related motion artifacts. **(b)** Abdominal image obtained with breath hold shows a minimal artifact due to respiration and several motion artifacts due to cardiac pulsation.

electromagnetic signal that could interfere with the MR signal. Leakage is usually caused by electronic equipment brought into the MR imaging room and the frequency generated by this equipment, which is picked up by the receive chain of the imager subsystem. The persistence of the problem even after the removal or electrical disconnection of all electronic equipment in the imager room might indicate that the RF shield has been compromised.

Motion-related Artifacts

Patient motion during image acquisition produces a commonly seen artifact. The artifact appears as blurring of the image as well as ghosting in the phase encoding direction. The time difference in the acquisition of adjacent points in the frequency encoding direction is relatively short (order of microseconds) and is dependent on the sampling frequency or the bandwidth used. The time difference in the acquisition of adjacent points in the phase encoding direction is much longer and is equal to the repetition time used for the sequence. The positional difference because of motion introduces a phase difference between the views in k-space that appears as a ghost on the image.

Respiratory and cardiac motion also can cause movement-related artifacts in the phase encoding direction. In general, periodic movements cause coherent ghosts, whereas nonperiodic movements cause a smearing of the image (15). Motion artifacts are generally caused by phase differences between adjacent k-space lines that are encoded at different phases of cardiac pulsation and respiration. Figure 7a shows an image affected by artifacts due to respiration. The best way to eliminate respiration-related motion is to perform breath-hold imaging (Fig 7b). However, the number of sections that can be obtained during a 20-second breath hold is limited. Multiple breath holds may be performed to increase coverage and obtain images in batches, but this requires cooperation from the patient. Some patients might have difficulty with breath holding. For such patients, respiratory gating may work better, with image acquisition performed at a certain phase of the respiratory cycle. The drawback of respiratory gating is that the acquisition time is increased. Another way to effectively reduce respiratory motion artifacts is to use respiratory compensation or phase reordering (also called respiratory-ordered phase encoding, or ROPE), whereby the phase encoding steps are ordered on the basis of the phase of the respiratory cycle (16). This technique allows a smooth phase variation across k-space and the limitation of variation to a single cycle of respiration instead of several cycles. Figure 8 shows an example of images acquired with and without respiratory motion compensation by using a fast SE sequence. Respiratory-ordered phase encoding works well in patients with regular respiratory cycles but not in those with irregular breathing.

Real-time navigator echo gating is an elegant non–breath-hold technique that can be used to compensate for several different types of motion (17) (Fig 9). With this technique, an echo from

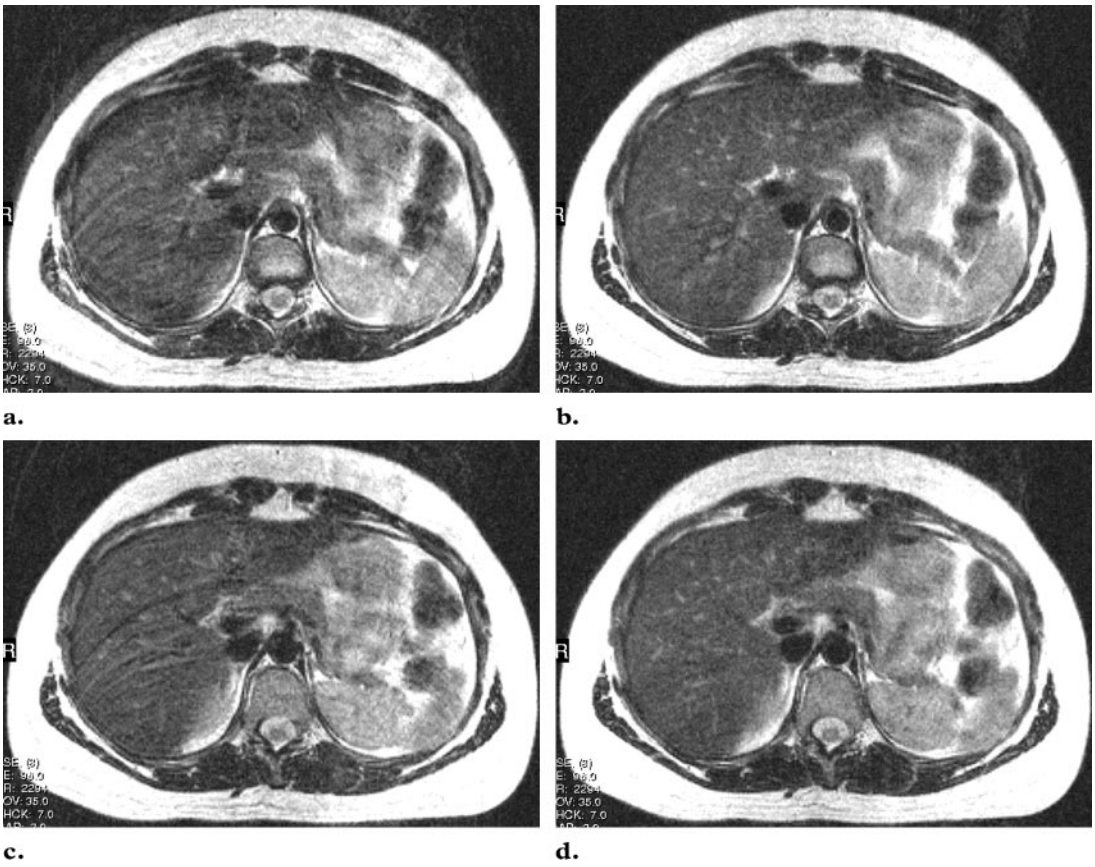

a. b. c. d.

Figure 8. Images acquired without and with compensation for respiratory motion. **(a, c)** Images acquired without compensation show respiration-induced artifact. **(b, d)** Images acquired with compensation are unaffected by respiratory motion.

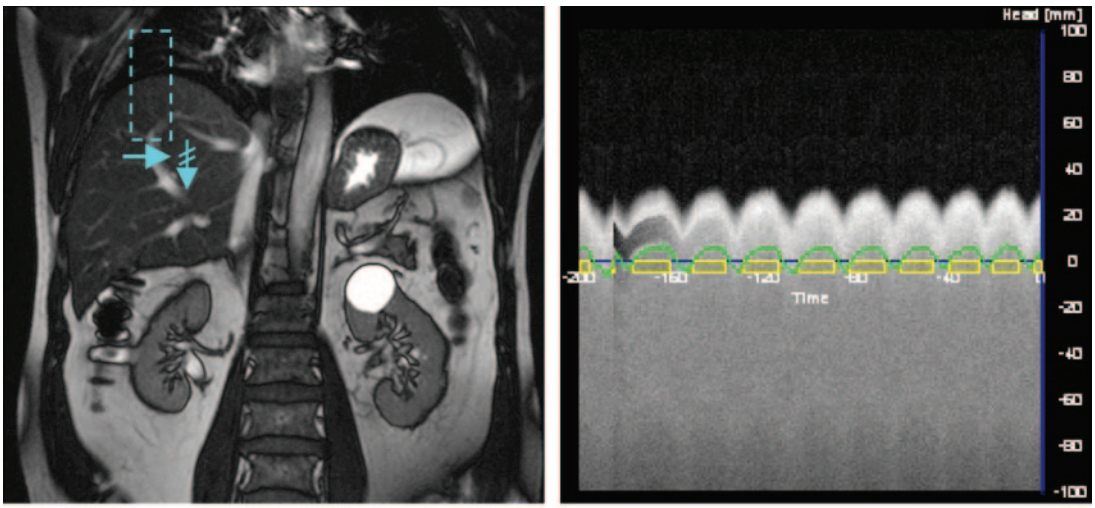

a. b.

Figure 9. Placement of the navigator section for respiratory motion compensation. **(a)** Image with aqua overlay shows the navigator section from which the displacement information is obtained to determine the diaphragmatic position. **(b)** Graph shows diagphragmatic movement, indicated by the white wave and green line. The yellow boxes represent the best time to image ("window of opportunity").

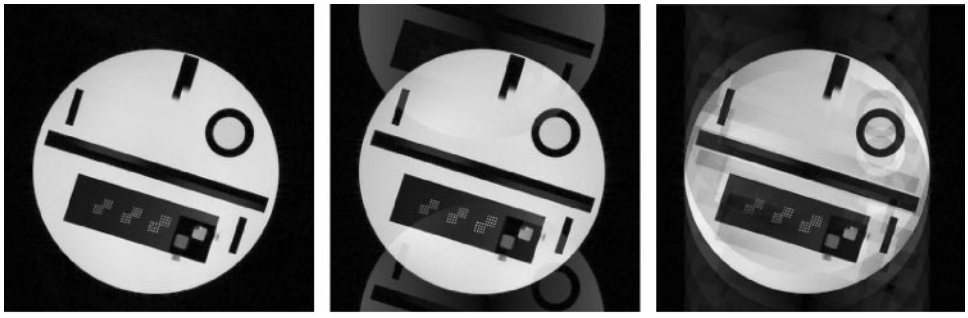

a. b. c.

Figure 10. Ghosts caused by phase errors at MR imaging in a phantom. **(a)** Initial image, acquired by using a fast SE sequence, shows no ghost artifact. **(b)** Image acquired with single-shot echo-planar imaging shows an N/2 ghost, a typical result of phase error (difference between odd- and even-numbered echoes). **(c)** Image acquired with a segmented-k-space MR sequence with eight phase-encoding lines per segment shows a coherent ghost.

the diaphragm is obtained to determine the diaphragmatic position, and the timing of the acquisition is adjusted so that data are acquired only during a specific range of diaphragmatic motion. The navigator echo part of the acquisition is interleaved with the actual imaging sequence to facilitate real-time monitoring.

Cardiac pulsation can also lead to motion artifacts, especially during imaging of the heart. Cardiac motion–related artifacts are avoided by using electrocardiographic gating to time image acquisition so that it occurs at the same phase of each cardiac cycle. Further artifact suppression can be achieved while imaging the heart if the acquisition is performed during breath holding.

N/2 Ghost and Segmented-k-Space Artifacts

Over the past few years, single-shot and multishot imaging sequences have been used increasingly in the clinical environment. Echo-planar imaging is based on the continuous reversal of the echoes by using a gradient pulse (commonly called gradient-recalled echo [GRE] imaging) after a single excitation for the acquisition of all lines in k-space to form a single image. In this case, every alternate line in k-space is read in the opposite direction because of the reversed polarity of the readout gradient. Prior to Fourier transform of the k-space data, these lines must be reversed. This reversal process may result in the introduction of phase errors in every alternate line of k-space. Phase errors can arise from minor deviations in the linear course of the gradient as it traverses from maximum positive polarity to maximum negative polarity, the existence of eddy currents in the system, or poor shimming. The mismatch in phase causes the appearance of ghosts on the reconstructed images. On images acquired with a single-shot echo-planar imaging sequence, the ghost appears as an additional image with reduced intensity that is shifted by half the field of view, as shown in Figure 10b, since half the lines of k-space are different from the other half. This type of ghost artifact is commonly referred to as an N/2 ghost. The minimization of phase errors helps reduce the intensity of the ghost image while enhancing the main image (18). A similar phenomenon occurs in multishot imaging sequences in which there is a phase discrepancy between the segments of k-space. The number of ghosts on the image increases with the number of discontinuities in the k-space, as illustrated by Figure 10c. On images acquired with a multishot sequence, errors could result from the number of echoes per shot and the number of segments in the k-space. To accurately correct for or minimize these artifacts, it may be necessary to obtain an additional navigator echo (18,19).

Images acquired with fast SE sequences also are susceptible to segmented-k-space artifacts. Here the discontinuities may occur because of a minor discrepancy in the timing of the sequence (eg, between the multiple RF pulses or between the data collection windows) or because of eddy currents within the system. Any of these items could easily introduce phase errors that result in ghosting. In most situations, a user can do nothing but call service support to address the problem.

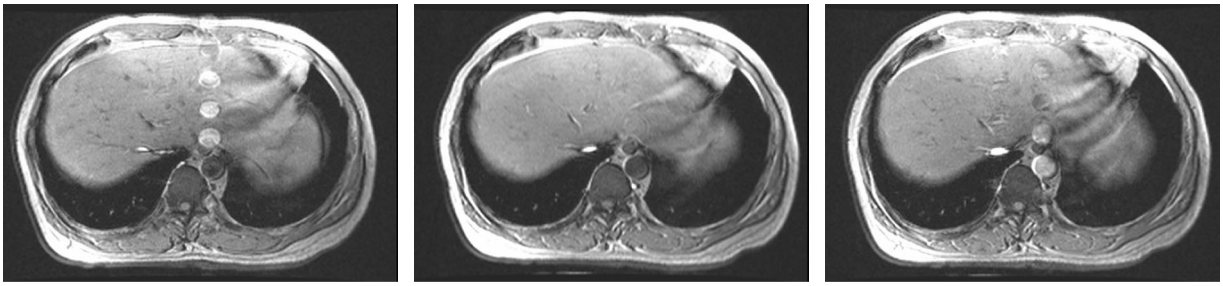

a. b. c.

Figure 11. Control of flow-related artifacts. **(a)** Image shows a cardiac pulsation artifact. **(b, c)** Images obtained with a saturation band superior to the imaging section **(b)** and with first-order motion compensation **(c)** show less severe flow-related artifacts.

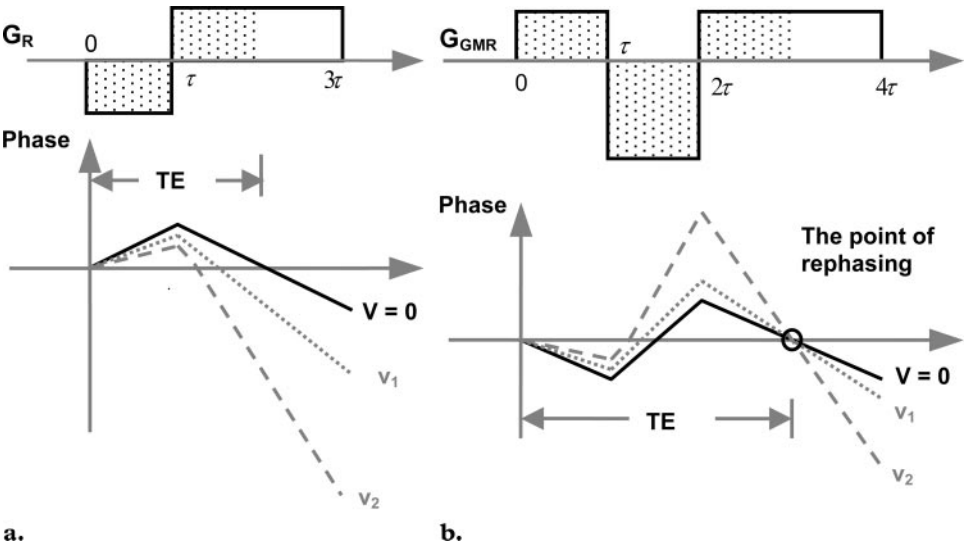

a. b.

Figure 12. Schematics show the MR signal effects of flow compensation with gradient moment nulling. Top: Typical readout gradient waveform. Bottom: Phase of cumulative stationary spins (solid line) and constant-velocity spins (dotted and dashed lines). **(a)** During imaging without flow compensation, the moving spins are not refocused at the desired echo time *(TE)*, and this leads to the loss of signal from flowing spins. **(b)** During imaging with gradient moment nulling, all the spins are refocused, and flow velocity is compensated for by the 1:2:1 ratio of the gradient lobe areas. G_{GMR} = gradient moment nulling gradient, G_R = readout gradient.

Flow Artifacts

Flowing blood is another source of motion-related artifacts, as shown in Figure 11. The blood flow is manifested as ghosting in the phase encoding direction. GRE sequences are much more susceptible to flow artifacts than are SE sequences. In SE sequences, the flow usually appears dark (produces no signal) because the flowing blood that is exposed to the 90° excitation pulse moves out of the imaging section before the refocusing 180° pulse is applied, while the blood that moved into the section at the same time was never exposed to the excitation pulse. In GRE imaging, the in-flow effect produces the bright-blood phenomenon. A common way to reduce the motion artifact caused by through-plane flow is to apply a saturation band adjacent to the imaging section. With this method, all spins within the slab are tilted toward the axial plane by a 90° RF pulse and then spoiled with the application of strong gradient crusher pulses before image acquisition starts. The spins, thus saturated, exhibit no signal when they move into the imaging volume (Fig 11b).

Flow artifacts could also be minimized by using flow compensation or gradient moment nulling. In this technique, flowing spins are rephased by using motion-compensating gradient pulses. As illustrated in Figure 12, if no motion

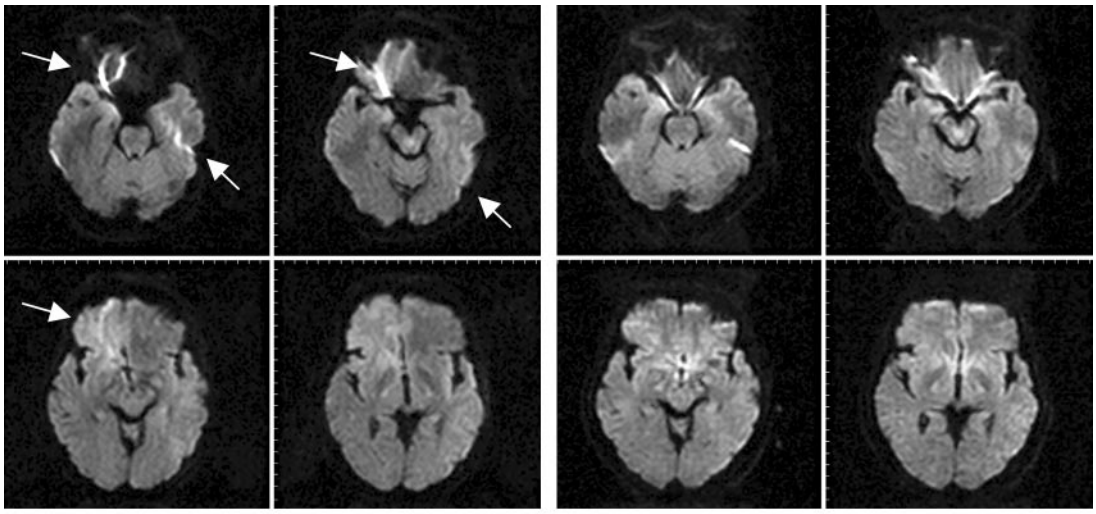

a. b.

Figure 13. Echo-planar images show magnetic susceptibility artifacts. **(a)** Left-right phase encoding causes severe distortion of the signal (arrows). **(b)** Anterior-posterior phase encoding minimizes the distortion, since the phase axis is symmetric around the susceptibility gradients.

compensation is applied with the gradients, the flowing spins are not in phase with the static spins when the echo forms. With motion compensation, the flowing spins with constant velocity (irrespective of what the velocity is) are brought back into phase, with no effect on static spins. Figure 11c illustrates the decrease in the severity of flow artifacts with the use of first-order motion compensation, in comparison with flow artifacts in Figure 11a, which was acquired without motion compensation. The penalty for using motion compensation is increased echo time. Higher-order motion compensation also can be obtained for spins with constant acceleration and for spins with varying acceleration (wobbling) by applying additional gradient pulses, but this increases the echo time even further (20).

Susceptibility Effects

When placed in a large magnetic field, tissues are temporarily magnetized, with the extent of the magnetization depending on the magnetic susceptibility of the tissue. The effect of tissue magnetization slightly alters the local magnetic field. The difference in tissue susceptibility causes field inhomogeneity between tissue boundaries, which makes spins dephase faster, producing signals of low intensity. This signal loss is especially severe at air-tissue or bone–soft tissue boundaries, because air and bone have much lower magnetic susceptibility than do most tissues. Local magnetic fields tend to take on different configurations around these interfaces, and the difference introduces geometric distortion into the resultant images, especially when sequences with long echo times are used. SE sequences are less affected by local field inhomogeneity because of the 180° refocusing pulse, which cancels the susceptibility gradients. Echo-planar images generally are subject to more severe susceptibility artifacts because the echoes are refocused by using gradient refocusing over a long period. Figure 13a shows a susceptibility artifact that occurred at echo-planar imaging. Note the distortion, near the air-tissue interface, that was caused by the susceptibility difference. One way to minimize this distortion is to orient the phase encoding gradient along the same axis as the susceptibility gradients. Figure 13a shows echo-planar images acquired with the phase encoding gradient in a left-right direction with regard to the image, whereas Figure 13b shows the same echo-planar images acquired with the phase encoding gradient in the anterior-posterior direction. Although the severity of the distortion is markedly reduced, there is still some residual distortion and some stretching in the direction of the phase encoding gradient. A good understanding of the anatomy and the types of tissues involved may help reduce susceptibility-related artifacts. The best way to minimize susceptibility artifacts is to use an SE sequence or reduce the echo time and increase the acquisition matrix. Proper shimming over the volume of interest before image acquisition is also critical to improve the local field homogeneity.

The artifact that is caused by the presence of metallic implants is of the same nature, but it is more severe because most metals have much higher magnetic susceptibility than does body

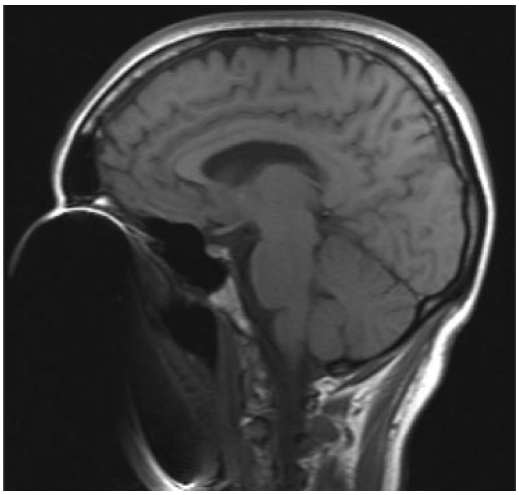

Figure 14. Sagittal MR image shows a magnetic susceptibility artifact that resulted from the presence of metallic dental fillings.

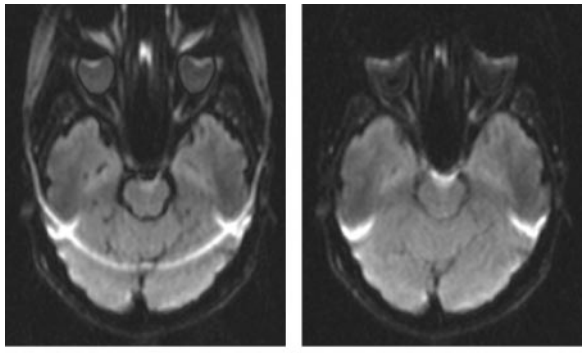

a. **b.**

Figure 15. Chemical shift artifact at echo-planar imaging. **(a)** Image shows severe chemical shift artifact from insufficient fat suppression. **(b)** Image obtained with fat saturation shows minimization of the chemical shift artifact or off-resonance effect.

tissue. As shown in Figure 14, metal-related artifacts typically are manifested as areas of complete signal loss because the local magnetic field is so strong that the spins are almost immediately dephased. Sometimes, depending on the strength of the resultant distortion of the magnetic field, part of a section may appear on images acquired in a completely different section because of the frequency difference between the spins in the metal and those next to the metal. The visual distortion created by metallic implants on MR images cannot be completely eliminated, but its effect can be minimized by a large receiver bandwidth and a decreased echo time. Fast SE acquisitions with a high bandwidth typically work well in such cases. However, care should be taken to avoid the heating of tissue that is adjacent to the metal (21).

Chemical Shift Artifacts

Protons in water and protons in fat have a significantly different chemical environment, which causes their resonance frequencies to differ. At 1.5 T, protons from fat resonate at a point approximately 220 Hz downfield from the water proton resonance frequency, and this difference in frequency is linearly related to magnetic field strength. The shift in Larmor frequency between water protons and fat protons is referred to as chemical shift. The suppression of fat protons at MR imaging is very useful for improving contrast on images of the breast, abdomen, and optic nerve (22).

The chemical shift between water and fat can cause artifacts in the frequency encoding direction. If this occurs, there will be a slight misregistration of the fat content on images, because of the slight shift in the frequency of the fat protons. The number of pixels involved in this slight shift depends on the receiver bandwidth and the number of data points used to encode the frequency direction. In mathematic terms, the result may be expressed as follows: $CSA = \Delta\omega \cdot N_{freq}/BW_{rec}$, where CSA is a chemical shift artifact, $\Delta\omega$ is the frequency difference between fat and water, N_{freq} is the number of samples in the frequency encoding direction, and BW_{rec} is the receiver bandwidth. This implies that the chemical shift can be minimized by using a higher receiver bandwidth.

Chemical shift artifacts were common on T2-weighted images obtained before the invention of fast SE imaging. The overall signal intensity on a normal T2-weighted image was low, and in order to increase the signal-to-noise ratio, it was a common practice to use a low receiver bandwidth for the T2-weighted echo. With the use of fast SE sequences, in contrast, the goals are to minimize the echo spacing and to maximize the decaying T2 signal. These goals are usually achieved by using a shorter RF pulse and a higher-bandwidth receiver window.

The signal from fat can dominate the dynamic range of an image and suppress the contrast between lesions and normal tissue, especially on abdominal MR images. Echo-planar images are very susceptible to artifacts from off-resonance frequencies, and unless the fat frequency is suppressed, the images will be degraded by fat-related artifacts. Any off-resonance signal (such as that of fat) will be affected by a position shift along the image because of the long duration of data sampling (50–100 msec). Such a shift could affect approximately 12 pixels at a readout time of 50 msec, as shown in Figure 15a. A common method for minimizing fat-related artifacts is to

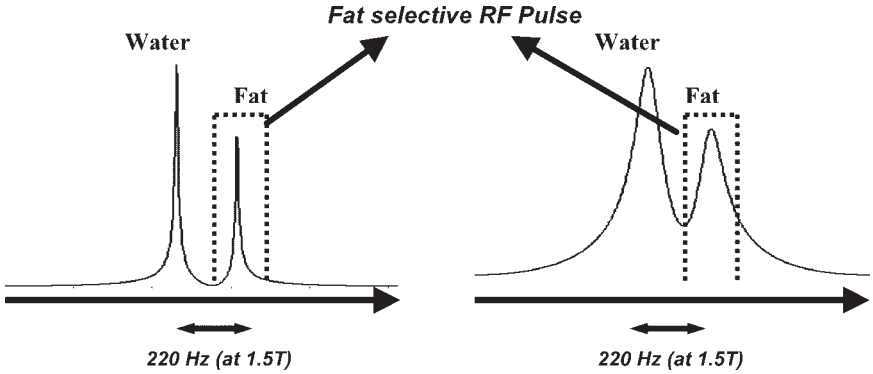

Figure 16. Schematics show the effect of fat saturation with an RF pulse applied at different frequencies for differentiation of water from fat. Left: Good magnetic field homogeneity, which results from a good shim, ensures effective fat suppression on images. Right: Poor homogeneity, or a bad shim, may produce nonuniform fat suppression on images and compromise the clinical reading.

apply a frequency-selective RF pulse to null the fat signal before applying the imaging pulse sequence (23). Successful fat saturation will result only if the magnetic field homogeneity is sufficient throughout the imaging region. Figure 16 illustrates the difference between a poorly shimmed object and a well-shimmed object at MR imaging with fat saturation. The result, in the case of the poorly shimmed object, is saturation not only of fat but also of a significant amount of water content; the resultant images are nondiagnostic. Therefore, it is necessary to properly shim the region before applying fat saturation. Proper shimming results in the depiction of two distinct signals in fat and in water. As shown in Figure 15b, good shimming, followed by fat saturation, enables the avoidance of off-resonance effects from fat. Another method is to use a short inversion time inversion recovery (STIR) sequence (24), as shown in Figure 17. In this method, the short T1 of the fat signal is used to suppress the signal from fat through the use of an inversion recovery sequence. If the T1 of any tissue is known, the inversion time needed to null the signal from that tissue in an inversion recovery sequence is given by 0.7 · T1. In the case of fat, the inversion time is around 150 msec at 1.5 T. The decision to use fat saturation or a STIR sequence depends on the specific application; both methods have advantages and disadvantages (25).

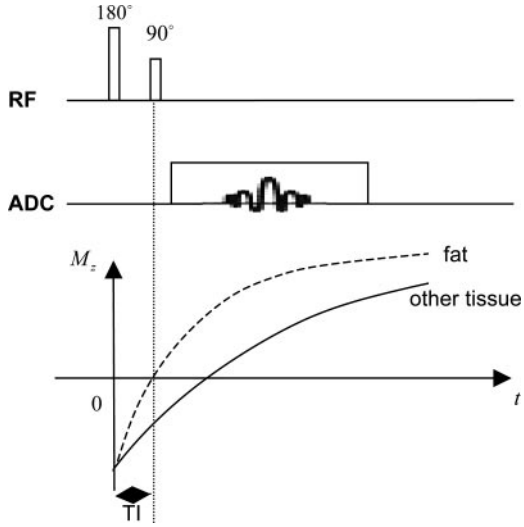

Figure 17. STIR sequence. The inversion time *(TI)* is set so that the available net magnetization of fat is zero at 0.7 · T1 of fat. *ADC* = analog-to-digital converter, M_z = longitudinal magnetization, *RF* = RF pulse.

In-phase versus Opposed-phase Imaging

Chemical shift can be used to advantage, as is routinely done in liver imaging for the detection of fatty infiltration. Because the precessional frequencies of fat and water are different, they go in and out of phase from each other after excitation. Since the difference in frequency between fat and water is about 220 Hz, the fat and water signals are in phase every 1/220 Hz. In other words, they are in phase at 4.45 msec, 8.9 msec, and so on (these time points correspond to the first cycle, second cycle, and later cycles). Within each cycle, the fat and water signals would be 180° out of phase with one another at 2.23 msec, 6.69 msec, and so on. Figure 18 shows the difference between in-phase and opposed-phase abdominal images obtained with echo times of 2.2 msec and 4.4 msec, respectively, at 1.5 T. At the in-phase echo times, the water and fat signals are summed within any pixel that contains a mixture of the two components, whereas at opposed-phase echo times, the signal in these pixels is canceled out, leading to the appearance of a dark band at the fat-water interface. In-phase and opposed-phase imaging sequences are sometimes also referred to as chemical shift sequences (26).

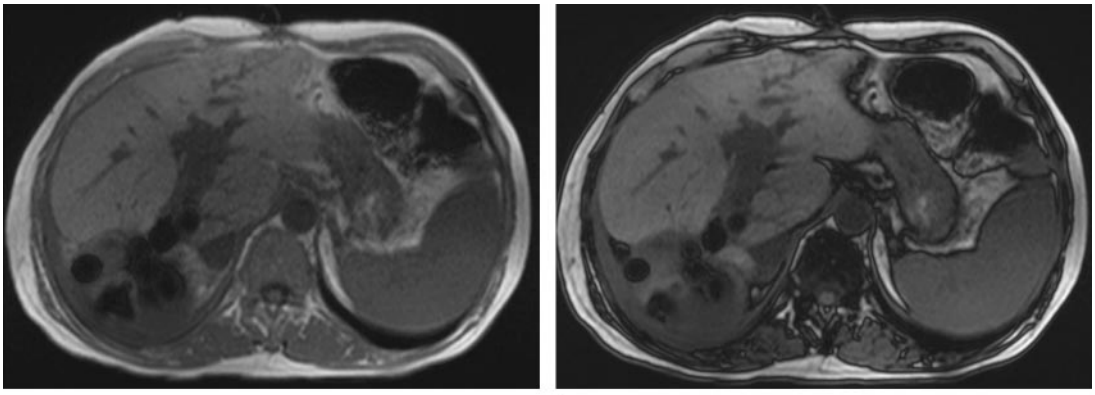

a. b.

Figure 18. **(a)** In-phase MR image acquired with an echo time of 2.2 msec. **(b)** Opposed-phase MR image acquired with an echo time of 4.4 msec. Both images were acquired at 1.5 T.

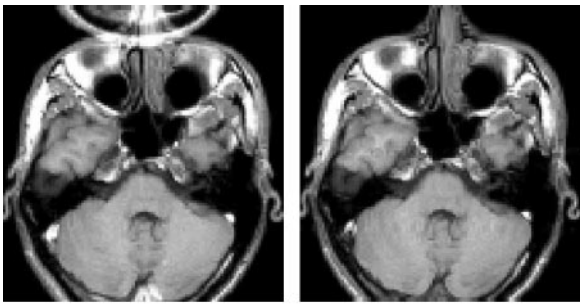

a. b.

Figure 19. Aliasing artifact caused by imaging with too small a field of view. **(a)** Image shows aliasing artifact. **(b)** Image obtained with the phase encoding and frequency encoding axes exchanged shows no aliasing.

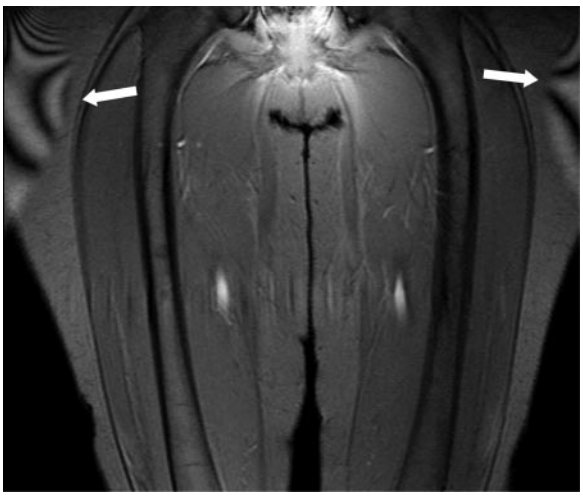

Figure 20. Aliasing artifact caused by phase errors at both sides of the magnet. Image shows a moiré artifact produced by the addition and cancellation of signals.

Aliasing (Wraparound) Artifacts

A common artifact routinely encountered in MR imaging is aliasing. Aliasing occurs whenever the imaging field of view is smaller than the anatomy being imaged. It should be noted that the field of view in both the readout and the phase encoding directions is inversely proportional to the incremental gradient step required from one point to the next. This means that the field of view is the distance along the gradient that one must move to experience one complete cycle. Therefore, when a field of view is selected, it is expected that the gradient will move one cycle ($0–2\pi$) from one end of the field to the other. If the sensitivity of the RF transmission coil extends beyond this field of view, the spins outside the field will be excited, but they will be part of the next cycle in the phase encoding direction (eg, $2–4\pi$, $4–6\pi$, and so on). However, the phase angles of the spins outside the field of view are essentially equivalent to those of the spins within the selected field of view but on the opposite side of the image. For the Fourier transform, spins at 10° are equivalent to spins at $2\pi + 10°$, and the result is an overlap of signals outside the intended field of view with signals within that field of view. Figure 19 shows aliasing of signals from outside the field of view in the imaging volume of interest. Aliasing is always encountered in the phase encoding direction because the frequency encoding direction is typically oversampled within the system. Aliasing also can occur in the section direction in a three-dimensional (3D) acquisition. In this case, the side lobes of the RF pulse that excites the 3D slab produce a signal from outside the field of view, and information in the first section may be aliased in the last section of a 3D acquisition.

Especially in the coronal plane, large fields of view that are smaller than the object will not only cause aliasing but also create an interference pattern called the moiré or fringe artifact. Homogeneity of the main field over large fields of view degrades toward the edges of the field, causing phase differences between the two edges. When aliasing occurs, the overlap of signals from one side of the body to the other side, with mismatched phases, produces a moiré artifact (Fig 20).

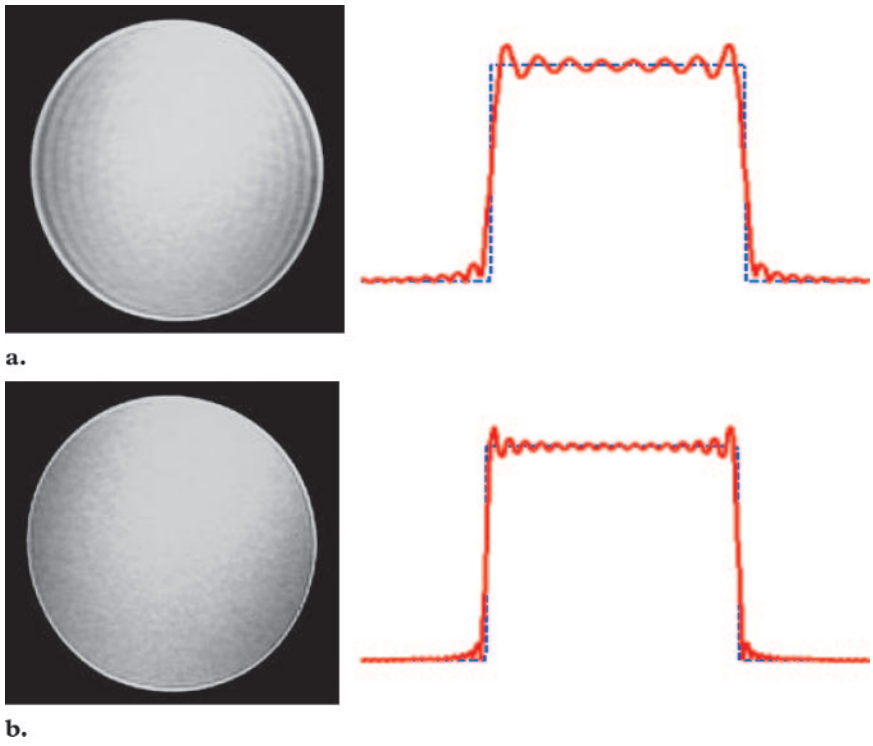

Figure 21. Gibbs ring artifact. **(a)** Axial image obtained with a low spatial resolution (128 × 128) in a cylinder shows a Gibbs ring artifact at the edges of the cylinder. **(b)** Image obtained with a higher spatial resolution (256 × 256) shows minimization of the artifact. The dotted line indicates the desired object profile, and the red line indicates the object profile with two different resolution parameters.

An easy way to eliminate aliasing is to exchange the readout direction with the phase encoding direction (swap the imaging axes) so that the anatomy fits into the phase field of view. However, this method may result in motion artifacts along the phase encoding direction that obscure a pathologic entity. Other ways of decreasing aliasing artifacts are to increase the phase field of view or to apply spatial saturation pulses outside the field of view so that the signals from outside the field of view will not give rise to artifacts within the field.

The interference pattern also occurs when different echoes from different excitation modes are received within the same acquisition window but with slightly different echo times. The second echo is often a stimulated echo. The spacing of the fringes in this case is inversely proportional to the difference in echo times. The only way to address this problem is either to adjust the timing of the sequence so that the stimulated echo is superimposed on the main echo or to use selective saturation to null the signal from the stimulated echo.

Gibbs Effect

Gibbs or truncation artifacts are bright or dark lines that appear parallel with and adjacent to the borders of an area of abrupt signal intensity change on MR images. Insufficient collection of samples in either the phase encoding direction or the readout direction leads to Gibbs rings as a result of the Fourier transform (27) (Fig 21). One usually sees Gibbs rings in the phase encoding direction because a phase encoding matrix that is smaller than the readout matrix is often selected to decrease the acquisition time. Gibbs rings can be minimized by increasing the acquisition matrix size and maintaining the same field of view, but the improvement comes with a penalty of increased acquisition time and a reduced per-pixel signal-to-noise ratio.

Section Cross Talk

Cross talk between sections occurs at imaging of contiguous sections (with no gap) in a multisection two-dimensional acquisition. Typically, in the presence of cross talk, all sections except the edge sections in a multisection acquisition have reduced signal intensity. The RF pulses used for excitation are not perfect in that they do not produce a section profile with a straight edge. In

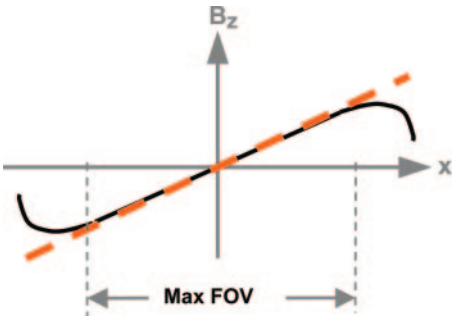

Figure 22. Schematic shows the geometric distortion of a typical gradient profile along the x-axis, with decreasing linearity (solid line) as the distance from the magnet isocenter increases. The red dotted line shows the desired linear gradient profile. B_z = magnetic field strength, *Max FOV* = maximum field of view.

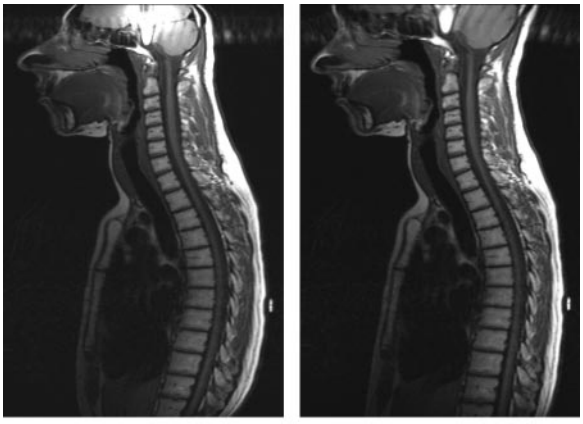

Figure 23. **(a)** SE image obtained with a large field of view shows the result of gradient geometric distortion. **(b)** Image obtained with a vendor-supplied correction algorithm shows correction of the geometric distortion.

addition, any side lobes to the RF pulse might excite the neighboring section by a few degrees. In other words, the neighboring section is subjected to an RF pulse more than once during a single repetition time, which causes partial saturation of the signal in that section and leads to a lower signal intensity. Possible remedies for cross talk between sections include RF pulses with sharper section profiles, an increased gap between sections, and/or multiple sections imaged in separate batches (one batch consisting of all the odd-numbered sections; the other, all the even-numbered sections). Three-dimensional images are not vulnerable to this effect because the whole volume undergoes excitation and because sections within the volume are acquired by using the gradients, as is the case with normal frequency and phase encoding.

Imaging System Cross Talk

Many imaging centers have more than one MR imaging system with the same field strength. If multiple MR imaging systems are operated at about the same frequency and at the same time, it is very important that each of the MR imaging rooms be surrounded by a tight shield to avoid cross talk between the imagers. It is probably best to ground the RF shield separately and keep the RF and gradient amplifiers for the individual imagers away from each other. To ensure that cross talk is not occurring, regular testing should be performed by applying intensive RF pulses and high-bandwidth reception on both imagers simultaneously.

Gradient-related Distortion

When an electrical current is applied to a gradient coil, a varying magnetic field is produced that is linear through the isocenter of the magnet but tapers toward the sides of the magnet. As illustrated in Figure 22, the gradient linearity gets worse with the distance from the isocenter. The effect of this distortion is to compress the images, thereby mismapping the spins from their true location at the edges of images obtained with a large field of view. Most MR imagers are equipped with distortion-correction algorithms to compensate for the gradient nonlinearity. Figure 23a shows the distortion on a spinal image with a large field of view, and Figure 23b shows the effect of the distortion-correction algorithm on the image. Because magnet sizes have become smaller in recent years, the possibility of geometric distortion should be given greater consideration, and the accuracy of correction algorithms should be assessed (28).

Parallel Imaging Artifact

New signal acquisition schemes such as SMASH (*sim*ultaneous *a*cquisition of *s*patial *h*armonics), SENSE (*sens*itivity *e*ncoding), and GRAPPA (*g*ener*a*lized *a*utocalibrating *p*artially *p*arallel *a*cquisitions), which are categorized as parallel imaging techniques (29–31), have spawned a whole new avenue for growth in MR imaging methods and applications. Techniques such as echo-planar imaging and fast SE sequences may benefit from the new reliance on spatial information from

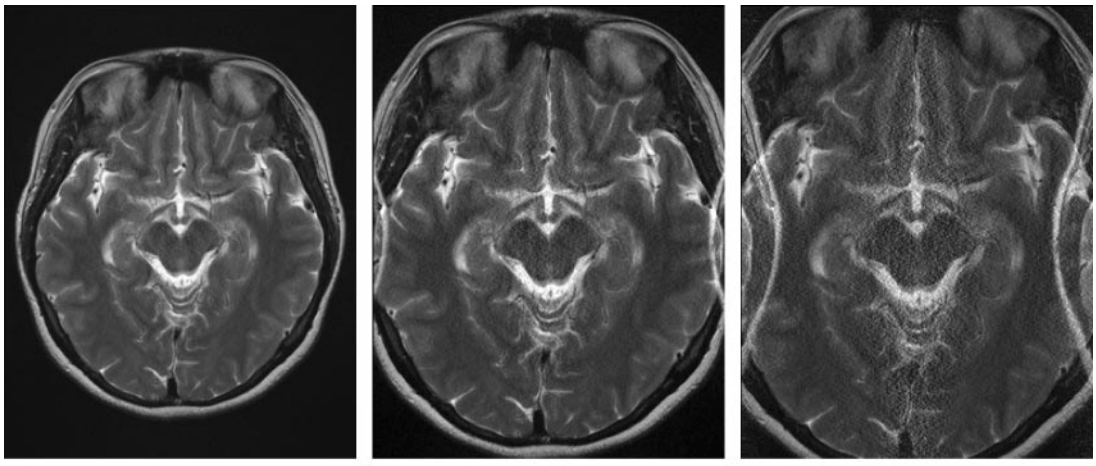

a. b. c.

Figure 24. Parallel imaging artifacts resulting from excessively small fields of view. A comparison of images acquired with a field of view of 22 cm **(a)**, 18 cm **(b)**, and 16 cm **(c)** and with a constant acceleration factor of two shows increasing severity of aliasing artifacts, as well as increasing noise at the image center, in **b** and **c**.

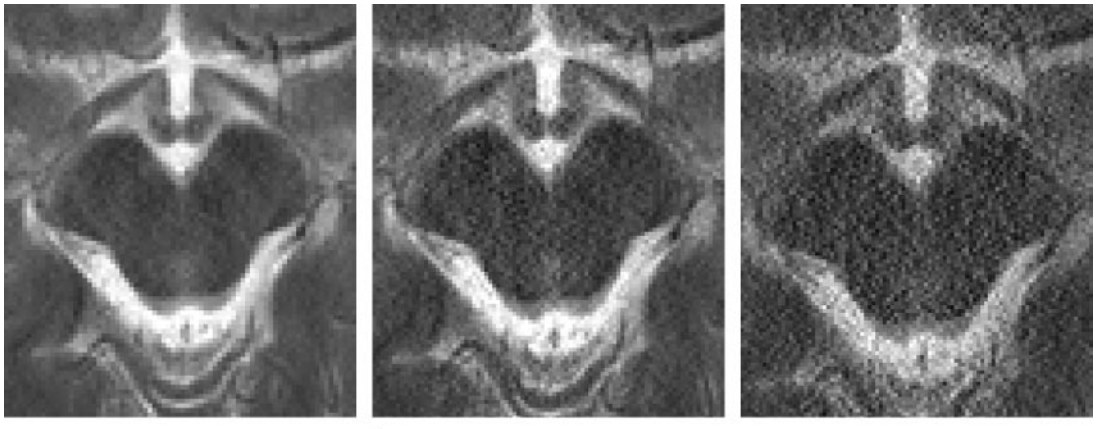

a. b. c.

Figure 25. Parallel imaging artifacts resulting from excessive acceleration factors. A comparison of images acquired at a constant field of view of 22 cm and with no acceleration **(a)**, with an acceleration factor of two **(b)**, and with an acceleration factor of three **(c)** shows a marked increase in noise and loss of resolution with increases in the acceleration factor.

phased-array coils to replace some of the spatial encoding performed with the usual gradient steps. Linear combinations of the sensitivities of the individual coils in an array are used to form spatial harmonics. These harmonics can be used to replace data obtained from some of the traditional phase encoding steps, thereby reducing the acquisition time. The reduced acquisition time can be used to improve spatial or temporal resolution. However, care must be taken to avoid the use of overaggressive acceleration factors or of fields of view smaller than the object being imaged. Parallel imaging artifacts differ from the routinely seen MR imaging artifacts. When the field of view is smaller than the object, aliasing artifacts can still occur, but additional artifacts appear in the center of the image (32). Figure 24 shows increased ghosting and noise in the center of the image with progressive reductions in the field of view. In addition, while temporal resolution can be improved with the use of acceleration factors greater than one, the overall magnitude and inhomogeneity of background noise increase with the acceleration factor, as shown in Figure 25 (33,34).

There are other artifacts that may be encountered in MR imaging, and it is impossible to list and discuss each one in this article. The artifacts described are those most frequently encountered, and a good understanding of the sources of these artifacts will lead to a better understanding of system performance and to more effective corrective action.

Teaching Point

MR Safety

MR safety issues are related to the three main subsystems within the MR imaging system. These are the static magnetic field, the time-varied magnetic field from the gradient subsystem, and the RF field from the RF subsystem. The magnetic field strengths of clinical MR imaging systems vary from 0.2 to 3.0 T. Static magnetic field strengths greater than 1.5 T may induce mild sensory effects when a person moves within the field. Time-varied gradient field strength (ie, the rate of change in the magnetic field, rendered in mathematic terms as dB/dt), which is measured in gauss per centimeter per second, may cause peripheral nerve stimulation. In addition, the RF field has the potential to heat tissue because the conductivity of the tissues supports the transfer of RF energy into conductive electricity within the tissue. Because of these potential biologic effects, the FDA has published guidelines for the safe operation of MR imaging systems. Manufacturers are mandated to ensure that their equipment operates in accordance with these guidelines, and proof of compliance is required by the FDA before any MR imaging system is approved (35).

Static Magnetic Fields

Most epidemiologic studies about the effect of static magnetic fields on the human body have been performed in populations of MR imaging technologists and other workers in a controlled environment. Investigators have focused on the long-term exposure of workers with electrolytic cells in chemical separation plants to a static magnetic field of very low strength (15.0-mT) or workers in various national research labs with short-term exposure to fields of up to 2.0 T (36–38). None have demonstrated a significant increase in any disease rate. Some creatures, such as bees and pigeons, are especially sensitive to variations in the magnetic field of the earth because of the magnetite content in their brains, which serves as an internal compass. Although no such structures have been identified in higher organisms or in humans, it is known that moving blood can induce electric potential on the order of millivolts within a static magnetic field. The so-called magnetohydrodynamic effect is not considered hazardous at the magnetic field strengths that are approved for clinical use. However, at higher field strengths, the probability exists that induced potential might exceed 40 mV, the threshold for depolarization of cardiac muscle. Despite very low or nonexistent risk from high-strength static magnetic fields, there are sporadic reports of headache, vomiting, hiccupping, numbness, and tinnitus, but they have not been substantiated. It should be noted that these sensory effects also were reported when the electrical current through the magnets was turned off. However, investigators in other studies have shown significant sensory effects (nausea, vertigo, and a metallic taste) at 4.0 T compared with 1.5 T. There also have been reports of an experience of flashing lights resulting from rapid movement in large magnetic fields. These lights, which are called magnetophosphenes, are thought to be caused by retinal stimulation by induced currents. In 1996, the FDA designated all field strengths of less than 4.0 T as posing a nonsignificant risk. Based on data obtained in humans at strengths of more than 4.0 T and in animals at as much as 16.0 T, this limitation for clinical magnets provides a substantial threshold for any adverse events that might arise from static fields (39,40).

Although exposure to magnetic fields may be safe, unsafe practices around the magnet have led to many accidents, some of them fatal. Access to the magnet room must be strictly controlled to prevent unintended subjects and personnel from being exposed to the high-strength magnetic field. Large signs should be posted to warn bystanders of the presence of a large magnetic field and the hazards associated with entering the magnet room. In addition, the nursing staff, technologists, radiologists, and other clinicians should be educated about the hazards of approaching a magnet. Precautions should be taken so that no person is able to take any metallic objects inside the magnet room, because such objects could become projectiles that might harm the patient on the imaging table. If the 5-gauss line falls outside the shielded magnet room, the area should be clearly marked and barricaded so that people with cardiac pacemakers do not enter this zone. A visible indicator of the 5-gauss line within the magnet room also is helpful for planning the placement of monitoring equipment and other apparatuses in the MR imaging room.

Prior to MR imaging examinations, technologists and clinicians also should carefully question patients about whether they have ferromagnetic implants such as surgical clips, coils, stents, and pacemakers. Because such implants are ferromagnetic, the static magnetic field may torque the object and exert a translational force. Most of the fatal accidents in MR imaging were caused by the failure to identify subjects with a cardiac pacemaker. The FDA recently received several reports of serious injury, including coma and permanent neurologic impairment in patients with neurologic stimulators, that occurred during an MR

imaging procedure. The most likely cause of such injury was heating of the electrodes at the end of the lead wires, which damaged the surrounding tissue. According to the FDA report, "Although these reports involved deep brain stimulators and vagus nerve stimulators, similar injuries could be caused by any type of implanted neurologic stimulator, such as spinal cord stimulators, peripheral nerve stimulators, and neuromuscular stimulators." If MR imaging is to be performed in a patient with an implanted neurologic stimulator, the documentation for the specific model that is implanted in the patient should be reviewed with particular attention to warnings and precautions (41). The radiologist may need to consult with the implanting or monitoring physician to obtain this information. In general, any instructions for MR imaging that are in the labeling for the implant, including information on types and/or strengths of MR imaging equipment that was tested for interaction with the particular implanted device, should be noted and followed exactly. The radiologist may need to consult with the device implant manufacturer for this information. The force fields generated by implants are more and more relevant as MR imagers with field strength of 3.0 T take a stronger hold in the marketplace. MR imaging personnel, including radiologists, therefore need to have the appropriate procedures in place to track patients with such implants before approving them for MR imaging. Shellock (42) provides an excellent reference list of implants for which MR imaging is contraindicated.

Time-varied Magnetic Fields

Spatial localization and encoding are achieved by using gradient coils that are inside the main magnet. The magnetic field generated by a gradient coil is extremely small, compared with the main magnetic field. The rate of change in the gradient field strength is expressed in milliteslas per meter per millisecond or in gauss per centimeter per second, and gradient field strengths as high as 45 mT/m with very rapid switching capabilities are now available for clinical use. Each orthogonal axis has a pair of gradient coils, and by applying electrical current in opposite directions to the coil loops, varying linear magnetic fields can be generated within the main magnetic field.

Just as the magnetic signal from nuclear precession induces a current that is picked up by the receiver coil, an electrical current and field may be induced in a patient with changing magnetic fields, as described by the Faraday law of induction (41). Normal imaging sequences induce currents of a few tens of milliamperes per square meter, a level that is far below that present in the normal brain and heart tissue. However, the rapid switching of magnetic field gradients that is produced with single-shot techniques such as echo-planar imaging is capable of generating currents that exceed the nerve depolarization threshold and cause peripheral nerve stimulation. The density of the induced current depends on the number of gradient switching operations per unit of time and on the rate of change of the magnetic field during each switching operation. The number of gradient switching operations per unit of time determines the duration of the current induced, while the rate of change in the magnetic field during each switching operation determines the maximum current induced (also referred to as the maximum slew rate) with a given gradient system (43).

The rate of change in the magnetic field (dB/dt) in MR imaging is classified as an extremely low frequency electromagnetic field. Biologic effects of extremely low frequencies emitted by transmission lines have received a lot of attention lately because the results of a number of epidemiologic studies suggested a weak negative link between extremely low frequency emissions and health. While many have questioned the design of those studies (because of the lack of matched controls, the absence of a dose-response relationship, or the absence of control for the effects of carcinogens), it should be remembered that they were performed in human subjects who were exposed to extremely low frequencies over very long periods. In comparison, the exposure to extremely low frequencies that is incurred in a single MR imaging examination is negligible (it is equal to or less than the background exposure). Other effects, such as magnetophosphenes, also have been reported for exposure to time-varied gradient fields (44–46).

The likelihood that peripheral nerve stimulation will occur is greatest during echo-planar imaging. This is especially true of acquisitions in oblique planes of section, since a higher slew rate results from the combined contributions of gradients from more than one axis. The likelihood of peripheral nerve stimulation is also greatest when the readout gradient at echo-planar imaging is in the craniocaudal direction.

Given that peripheral nerve stimulation is likely to occur with the use of techniques such as

echo-planar imaging, the FDA, adapting the standards of the International Electrotechnical Commission (technical report no. 60601–2-33), specified three modes of operation for time-varied magnetic fields. The normal mode, which is used for routine imaging of patients, is limited to 20 T/sec for gradient ramp time exceeding 120 μsec, for a total of less than 2400 T/sec (with ramp time between 12 and 120 μsec). The upper limit for the first controlled mode is 60,000 T/sec to prevent cardiac stimulation. This limit is unlikely to be reached by any of the commercial scanners. The second controlled mode can be used only for research and with the approval of an institutional review board. Current safety standards do adequately address the safety of patients and personnel. All MR imaging systems automatically monitor the rate of change in the magnetic field and provide warnings about the likelihood of peripheral nerve stimulation. Proper communication with patients should help alleviate further any concerns that the patient undergoing MR imaging may have (47,48).

Acoustic Noise

The pulsed currents that are passed through the gradient coils produce a torque on the coil itself and result in the movement of the gradient coils against their mountings. This movement, much like that of the diaphragm of a loudspeaker, creates the loud banging noises heard by the subject during MR imaging. The FDA follows the advice of the International Electrotechnical Commission, which essentially asks the manufacturer to provide a warning if the acoustic noise from a given pulse sequence is likely to exceed 99 dB(A), which is sufficiently removed from 140 dB(A), the level at which damage to the hearing may occur. Wearing proper headgear for hearing protection is extremely important during MR imaging and can lower noise levels by about 30 dB(A). Manufacturers of MR imaging systems are actively working to further decrease noise levels by using methods such as active noise cancellation filters and vacuum packing (49).

RF Energy

Prolonged exposure of biologic tissues to RF energy may result in tissue heating. The conductivity of the tissue allows the absorption of RF energy, which results in heating. This energy absorption is described in terms of the specific absorption rate. Such heating, if not controlled, can have physiologic effects such as changes in mental function and cardiac output. A rise in core body temperature by less than 1°C generally is no cause for concern, because cell death does not occur until the temperature exceeds 42°C. At temperatures of less than 42°C, autonomic response mechanisms in the body reverse any of the changes that occur with a temperature increase beyond normal levels (50). However, care should be taken when imaging patients with metallic objects (ferromagnetic or otherwise), which may result in increased heating compared with heating in normal biologic tissues. Failure to use MR-compatible leads during electrocardiographically gated cardiac MR imaging could result in skin burns.

The specific absorption rate is measured in watts per kilogram. Because the imaging system computer calculates the specific absorption rate on the basis of the weight value entered in the system, the correct weight of the subject must be entered during the patient registration process. The FDA limit for a permissible increase in body core temperature during MR imaging is 1°C. In addition, the FDA considers a significant risk to be incurred if the specific absorption rate exceeds 3 W/kg averaged over the head for 10 minutes, 4 W/kg averaged over the whole body for 15 minutes, 8 W/kg per gram of tissue averaged over the head or torso for 5 minutes, or 12 W/kg averaged over the extremities for 15 minutes (51).

It should be noted that the specific absorption rate increases with the square of the frequency and, hence, depends on magnetic field strength. With MR imaging at 3.0 T, a subject will experience nine times the specific absorption rate experienced with MR imaging at 1.0 T. The specific absorption rate increases with the square of the flip angle, the size of the patient, and the duty cycle of the RF pulses. The MR imager operator can minimize heat deposition by controlling the flip angle of the pulse, increasing the repetition time, decreasing the number of sections for a given repetition time, increasing the echo spacing in a fast SE sequence, decreasing the number of echoes in a fast SE sequence, and reducing the refocusing flip angle in a fast SE sequence. In general, the key to decreasing the specific absorption rate is to decrease both the power and the duty cycle of the RF pulses. This implies that protocols based on RF energy–intensive sequences or protocols for higher-field-strength magnets must be optimized to remain within the specific absorption rate limits while producing images with the desired level of contrast resolution.

Quality Control

When an institution or a clinic makes a substantial capital investment in an MR imaging system, it counts on reaping benefits from that investment for a long time. To obtain those dividends, a good quality-control or quality-assurance program is essential. Dividends are directly related to patient referrals, and referrals in turn depend on the reliability of MR imaging and the image quality at the particular site. In a complex system such as the MR imager, many things can go wrong. There could be a catastrophic failure of the entire system or a problem caused by one of the subsystems. Electrical and electronic components could gradually deteriorate, and if the deterioration goes undetected, it could lead to substantial imager downtime. Even a seemingly benign undertaking such as upgrading of software might change the characteristics of the imaging system in ways that could go undetected unless appropriate testing is performed before and after the upgrade.

Ideally, after the installation of a new system or upgrading of an existing system, the system should be evaluated by a physicist or a qualified engineer prior to use. The qualified engineer is usually the service engineer from the vendor of the MR imaging system who performs all the tests and provides a report to the customer (52,53). Acceptance testing is performed with MR imaging of phantoms to obtain information about various imaging parameters. Qualified personnel from within the respective MR imaging centers can use the test reports as a guideline in instituting a quality-control plan that tracks the various parameters over time. The parameters that are tracked should provide an indication of the overall stability of the system as well as of the various RF coils and should point toward any deviations from the norm in any subsystem. System stability could be measured by tracking the homogeneity of the magnetic field, signal-to-noise ratio, resolution, and contrast-to-noise ratio in a standard phantom. Such data should be collected on a periodic basis. The length of the interval between such tests may vary from site to site; testing should be accommodated realistically in the overall schedule, without increasing the burden on technologists or taking up too much time. The periodic collection of data alone is not enough: Only the results of regular analyses of the data can point toward a trend in the performance of the MR imaging system or its subsystems and allow the measurement of performance against threshold specifications. Trend analysis enables preventive maintenance of important components that may fail, thereby preventing substantial system downtime (54).

Most people agree that a quality-control program is beneficial for the smooth operation of an MR imaging system. However, very few sites implement rigorous quality control measures. To ensure a uniform quality of diagnosis across all MR imaging centers and all MR imaging system vendors, the ACR instituted an MR system accreditation program in 1996. Furthermore, it is the goal of the ACR to ensure that sites have a long-standing commitment to quality control. Participation in the ACR accreditation program is voluntary. The program is designed to be educational while providing a framework for quality control. It also includes an evaluation of the qualifications of technologists, radiologists, and other personnel who will read images from the system that is to be accredited, as well as evaluation of the equipment performance and the quality of clinical images. The accreditation process involves the purchase of a standardized phantom, and discounts for the accreditation process are available if an imaging center has more than one MR imaging system. There are seven quantitative measures that the ACR is looking for that can be determined from the ACR phantom images. These include geometric accuracy, spatial resolution of high-contrast objects, section thickness accuracy, section position accuracy, image intensity uniformity, percentage of signal ghosting, and low-contrast object detectability (55) (Fig 26). Accreditation is valid for 3 years and is renewable. A newly instituted regulation requires that new applicants and previously accredited sites submit an annual MR imaging system performance evaluation form, to be completed by a medical physicist or MR scientist. In addition, sites must submit copies of their weekly data from onsite quality-control testing for the most recent quarter (55,56).

Teaching Point

It is highly recommended that all sites apply for ACR accreditation, for the simple reason that the process of accreditation provides a means of establishing a quality-assurance or quality-control program that is recognized by leading authorities. An even more important and more practical reason to seek accreditation is that more and more insurance companies (starting with Aetna in 2001) require that sites be accredited before claims are submitted for insurance payment. The initial application process may seem daunting, but accreditation is well worth the effort. For

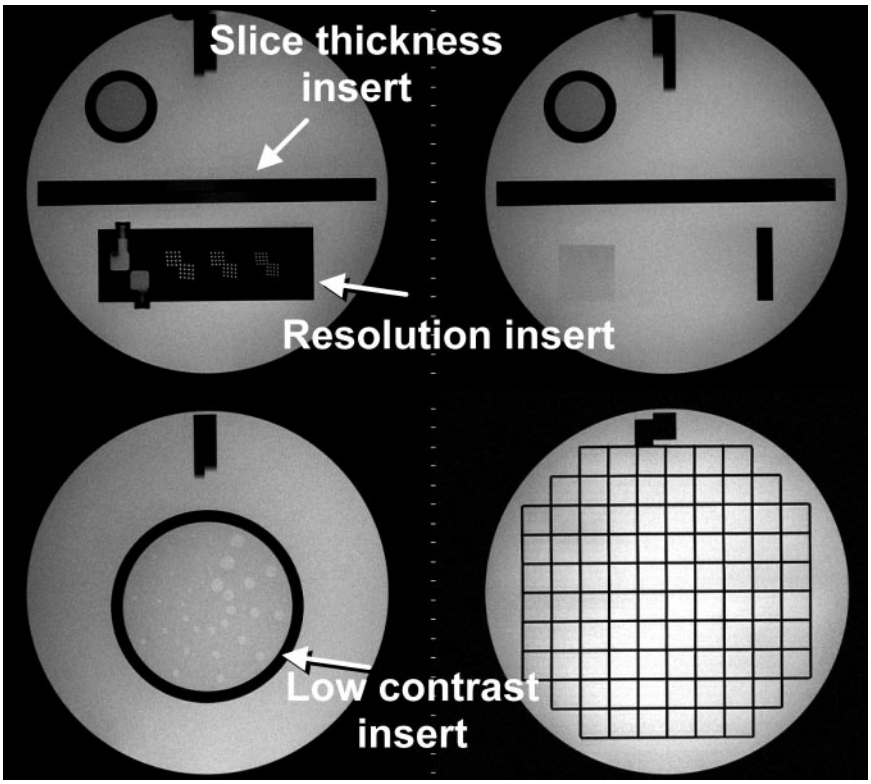

Figure 26. Images show the various inserts in the ACR phantom that are used to provide information about geometric accuracy, including the accuracy of the section thickness and section position, spatial resolution of high-contrast objects (top left), the percentage of signal ghosting, the detectability of low-contrast objects (bottom left), and the uniformity of image intensity (bottom right).

those who find the application process too time consuming, MR imaging system vendors and a number of consultants will provide the service for a fee. Although the quality-assurance process instituted by the ACR may enhance the smooth running of an MR imaging center, it might not help identify the cause of increased ghosting on echo-planar images or help resolve patient monitoring unit issues. However, the ACR quality-assurance guidelines can serve as the skeleton for a quality-control task list, to which individual sites may add items specific to their needs. Overall, following the ACR guidelines and conducting regular internal analyses of the data collected will enable imaging sites to achieve and maintain high standards of MR imaging quality.

Conclusions

MR imaging is a versatile and important modality for the diagnosis of various pathologic entities. A quality-control program that incorporates safe practices in the MR imaging environment and that reflects a good understanding of methods for avoiding artifacts will ultimately enable improvements in the efficiency of the use of this technology and, more important, in patient care.

References

1. Lauterbur PC. Image formation by induced local interactions: examples employing nuclear magnetic resonance. (1973.) Clin Orthop Relat Res 1989;244:3–6.
2. Lewin JS, Laub G, Hausmann R. Three-dimensional time-of-flight MR angiography: applications in the abdomen and thorax. Radiology 1991;179: 261–264.
3. Petitjean C, Rougon N, Cluzel P. Assessment of myocardial function: a review of quantification methods and results using tagged MRI. J Cardiovasc Magn Reson 2005;7:501–516.
4. McKnight TR. Proton magnetic resonance spectroscopic evaluation of brain tumor metabolism. Semin Oncol 2004;31:605–617.
5. Tofts PS. Modeling tracer kinetics in dynamic Gd-DTPA MR imaging. J Magn Reson Imaging 1997; 7:91–101.
6. Ogawa S, Tank DW, Menon R, et al. Intrinsic signal changes accompanying sensory stimulation: functional brain mapping with magnetic resonance imaging. Proc Natl Acad Sci U S A 1992;89: 5951–5955.
7. Hayes CE, Hattes N, Roemer PB. Volume imaging with MR phased arrays. Magn Reson Med 1991;18:309–319.

8. Sodickson DK, McKenzie CA, Ohliger MA, Yeh EN, Price MD. Recent advances in image reconstruction, coil sensitivity calibration, and coil array design for SMASH and generalized parallel MRI. MAGMA 2002;13:158–163.
9. Mansfield P. Multi-planar image formation using NMR spin echoes. J Phys C 1977;10:L55–L58.
10. Hennig J, Nauerth A, Friedburg H. RARE imaging: a fast method for clinical MR. Magn Reson Med 1986;3:823–833.
11. Mezrich R. A perspective on k-space. Radiology 1995;195:297–315.
12. Twieg DB. The k-trajectory formulation of the NMR imaging process with applications in analysis and synthesis of imaging methods. Med Phys 1983;10:610–621.
13. Hennig J. Generalized MR interferography. Magn Reson Med 1990;16:390–402.
14. Axel L, Montillo A, Kim D. Tagged magnetic resonance imaging of the heart: a survey. Med Image Anal 2005;9:376–393.
15. Wood ML, Henkelman RM. Magnetic resonance artifacts from periodic motion. Med Phys 1985; 12:143–151.
16. Bailes DR, Gilderdale DJ, Bydder GM, Collins AG, Firmin DN. Respiratory ordered phase encoding (ROPE): a method for reducing respiratory motion artifacts in MR imaging. J Comput Assist Tomogr 1985;9:835–838.
17. Ehman RL, Felmlee JP. Adaptive technique for high-definition MR imaging of moving structures. Radiology 1989;173:255–263.
18. Butts K, Riederer SJ, Ehman RL, Thompson RM, Jack CR. Interleaved echo planar imaging on a standard MRI system. Magn Reson Med 1994; 31:67–72.
19. McGee KP, Felmlee JP, Manduca A, Riederer SJ, Ehman RL. Rapid autocorrection using prescan navigator echoes. Magn Reson Med 2000;43:583–588.
20. Pattany PM, Phillips JJ, Chiu LC, et al. Motion artifact suppression technique (MAST) for MR imaging. J Comput Assist Tomogr 1987;11:369–377.
21. Kolind SH, MacKay AL, Munk PL, Xiang QS. Quantitative evaluation of metal artifact reduction techniques. J Magn Reson Imaging 2004;20:487–495.
22. Hood MN, Ho VB, Smirniotopoulos JG, Szumowski J. Chemical shift: the artifact and clinical tool revisited. RadioGraphics 1999;19:357–371.
23. Farzaneh F, Riederer SJ, Pelc NJ. Analysis of T2 limitations and off-resonance effects on spatial resolution and artifacts in echo-planar imaging. Magn Reson Med 1990;14:123–139.
24. Bydder GM, Young IR. MR imaging: clinical use of the inversion recovery sequence. J Comput Assist Tomogr 1985;9:659–675.
25. Nakatsu M, Hatabu H, Itoh H, et al. Comparison of short inversion time inversion recovery (STIR) and fat-saturated (chemsat) technique for background fat intensity suppression in cervical and thoracic MR imaging. J Magn Reson Imaging 2000;11:56–60.
26. Mitchell DG, Kim I, Chang TS, et al. Fatty liver: chemical shift phase-difference and suppression magnetic resonance imaging techniques in animals, phantoms and humans. Invest Radiol 1991; 26:1041–1052.
27. Bracewell R. The Fourier transform and its applications. New York, NY: McGraw-Hill, 1978.
28. Doran SJ, Charles-Edwards L, Reinsberg SA, Leach MO. A complete distortion correction for MR images. I. Gradient warp correction. Phys Med Biol 2005;50:1343–1361.
29. Sodickson DK, Manning WJ. Simultaneous acquisition of spatial harmonics (SMASH): fast imaging with radiofrequency coil arrays. Magn Reson Med 1997;38:591–603.
30. Pruessmann KP, Weiger M, Scheidegger MB, Boesiger P. SENSE: sensitivity encoding for fast MRI. Magn Reson Med 1999;42:952–962.
31. Griswold MA, Jakob PM, Heidemann RM, et al. Generalized autocalibrating partially parallel acquisitions (GRAPPA). Magn Reson Med 2002; 47:1202–1210.
32. Goldfarb JW. The SENSE ghost: field-of-view restrictions for SENSE imaging. J Magn Reson Imaging 2004;20:1046–1051.
33. Larkman DJ, Atkinson D, Hajnal JV. Artifact reduction using parallel imaging methods. Top Magn Reson Imaging 2004;15:267–275.
34. Bammer R, Schoenberg SO. Current concepts and advances in clinical parallel magnetic resonance imaging. Top Magn Reson Imaging 2004; 15:129–158.
35. Food and Drug Administration (FDA), Center for Devices and Radiological Health, Computed Imaging Devices Branch, Office of Device Evaluation. Guidance for the submission of premarket

notifications for magnetic resonance diagnostic devices. Web site of the FDA. http://www.fda.gov/cdrh/ode/mri340.pdf. Published November 14, 1998. Accessed November 17, 2005.
36. Marsh JL, Armstrong TJ, Jacobson AP, Smith RG. Health effect of occupational exposure to steady magnetic fields. Am Ind Hyg Assoc J 1982; 43:387–394.
37. Tenford TS, Budinger RF. Biological effects and physical safety aspects of NMR imaging and in vivo spectroscopy. In: Thomas SR, Dixon RL, eds. NMR in medicine: the instrumentation and clinical applications. Medical Physics Monograph no. 14. College Park, Md: American Institute of Physics, 1986; 493–548.
38. Sahl J, Mezei G, Kavet R, et al. Occupational magnetic field exposure and cardiovascular mortality in a cohort of electric utility workers. Am J Epidemiol 2002;156:913–918.
39. Schenck JF. Safety of strong, static magnetic fields. J Magn Reson Imaging 2000;12:2–19.
40. Formica D, Silvestri S. Biological effects of exposure to magnetic resonance imaging: an overview. Biomed Eng Online 2004;3:11.
41. Food and Drug Administration (FDA). Public health notification: MRI-caused injuries in patients with implanted neurological stimulators. Web site of the FDA. http://www.fda.gov/cdrh/safety/neurostim.html. Published May 10, 2005. Accessed November 17, 2005.
42. Shellock FG. Pocket guide to MR procedures and metallic objects: update 2001. Baltimore, Md: Lippincott Williams & Wilkins, 2001.
43. Ham CL, Engels JM, van de Wiel GT, Machielsen A. Peripheral nerve stimulation during MRI: effects of high gradient amplitude and switching rates. J Magn Reson Imaging 1997;7:933–937.
44. Theriault G, Goldberg M, Miller AB, et al. Cancer risks associated with occupational exposure to magnetic fields among electric utility workers in Ontario and Quebec, Canada, and France: 1970–1989. Am J Epidemiol 1994;139:550–572. [Published correction appears in Am J Epidemiol 1994; 139:1053.]
45. Villeneuve PJ, Agnew DA, Johnson KC, Mao Y. Canadian Cancer Registries Epidemiology Research Group. Brain cancer and occupational exposure to magnetic fields among men: results from a Canadian population-based case-control study. Int J Epidemiol 2002;31:210–217.
46. Bracken TD, Patterson RM. Variability and consistency of electric and magnetic field occupational exposure measurements. J Expo Anal Environ Epidemiol 1996;6:355–374. [Published corrections appear in J Expo Anal Environ Epidemiol 1996;6(4):527, J Expo Anal Environ Epidemiol 1997;7:553.]
47. Schaefer DJ, Bourland JD, Nyenhuis JA. Review of patient safety in time-varying gradient fields. J Magn Reson Imaging 2000;12:20–29.
48. International Electrotechnical Commission. Particular requirements for the safety of magnetic resonance equipment for medical diagnosis. In: Diagnostic imaging equipment. Publication no. 60601–2–33. Medical electrical equipment. Geneva, Switzerland: International Electrotechnical Commission, 1995.
49. McJury M, Shellock FG. Auditory noise associated with MR procedures: a review. J Magn Reson Imaging 2000;12:37–45.
50. Roberts NJ Jr, Michaelson SM, Lu ST. The biological effects of radiofrequency radiation: a critical review and recommendations. Int J Radiat Biol Relat Stud Phys Chem Med 1986;50:379–420.
51. Shellock FG. Radiofrequency energy-induced heating during MR procedures: a review. J Magn Reson Imaging 2000;12:30–36.
52. Lerski RA, McRobbie DW, Straughan K, Walker PM, de Certaines JD, Bernard AM. Multi-center trial with protocols and prototype test objects for the assessment of MRI equipment. EEC Concerted Research Project. Magn Reson Imaging 1988;6:201–214.
53. Och JG, Clarke GD, Sobol WT, Rosen CW, Mun SK. Acceptance testing of magnetic resonance imaging systems: report of AAPM Nuclear Magnetic Resonance Task Group No. 6. Med Phys 1992; 19:217–229.
54. McRobbie DW, Quest RA. Effectiveness and relevance of MR acceptance testing: results of an 8 year audit. Br J Radiol 2002;75:523–531.
55. American College of Radiology (ACR). MRI Accreditation Program requirements. Web site of the ACR. http://www.acr.org/s_acr/sec.asp?CID=1744&DID=12150&DOC=FILE.PDF. Published September 21, 2005. Accessed November 17, 2005.
56. American College of Radiology (ACR). Phantom test guidance for the ACR MRI Accreditation Program. Reston, Va: ACR, 1998.

Teaching Points for AAPM/RSNA Physics Tutorial for Residents: MR Artifacts, Safety, and Quality Control

Jiachen Zhuo, MS and Rao P. Gullapalli, PhD

RadioGraphics 2006; 26:275–297 • **Published online** 10.1148/rg.261055134 • **Content Codes:** MR PH QA

Page 276
We no longer look to MR imaging to provide only structural information, but also functional information of various kinds. Information about blood glow, cardiac function, biochemical processes, tumor kinetics, and blood oxygen levels (for mapping of brain function) are just a few examples of the data that can be obtained with MR imaging today (2–6).

Page 277
System-related artifacts might be due to transient effects generated within one or more of the subsystems or could be a sign of degradation of some of the electronic components in the subsystem. System-related artifacts can be minimized through the adoption of a good quality assurance or quality control program, such as the one recommended by the ACR. Artifacts related to physiology are dependent on complex interactions between the subject and the MR imaging system.

Page 278
Fourier transform of k-space is then applied to convert the data into an image. Each pixal in the resultant image is the weighted sum of all the individual points in k-space. Therefore, the information in each pixel is derived from a fraction of every point in k-space. On the basis of these facts, we can conclude that nay disruption of k-space, whether by motion, extraneous frequencies, or frequency spikes, has the potential to corrupt the entire image.

Page 291
The magnetic field strengths of clinical MR imaging systems vary from 0.2 to 3.0 T. Static magnetic field strengths grater than 1.5 T may induce mild sensory effects when a person moves within the field. Time-varied gradient field strength (ie, the rate of change in the magnetic field, rendered in mathematic terms as dB/dt), which is measured in gauss per centimeter per second, may cause peripheral nerve stimulation. In addition, the RF field has the potential to heat tissue because the conductivity of the tissues supports the transfer of RF energy into conductive electricity within the tissue.

Page 294
It is highly recommended that all sites apply for ACR accreditation, for the simple reason that the process of accreditation provides a means of establishing a quality-assurance or quality-control program that is recognized by leading authorities. An even more important and more practical reason to seek accreditation is that more and more insurance companies (starting with Aetna in 2001) require that sites be accredited before claims are submitted for insurance payment.